Simple, Inexpensive, and Rapid Approach to Fabricate Cross-Shaped Memristors Using an Inorganic-Nanowire-Digital-Alignment Technique and a One-Step Reduction Process

*Wentao Xu, Yeongjun Lee, Sung-Yong Min, Cheolmin Park, and Tae-Woo Lee**

Resistive random-access memory (RRAM) is a candidate fast high-density low-power-consumption memory structure due to its nonvolatility, high access speed, high density, and ease of fabrication.[1–7] Especially, cross-point access allows cross-bar arrays that lead to high-density cells in a 2D planar structure.[8–10] Use of such designs could be compatible with the aggressive scaling down of memory devices,[11] but existing methods to fabricate RRAM are too complicated. RRAM is usually fabricated using conventional optical or e-beam lithographic approaches.[12] Conventional deposition-lithographic approaches usually entail complicated etching steps, during which special attention should be paid to the separate deposition and patterning of the oxide layer in the metal–oxide–metal (MOM) structure.

1D inorganic nanowires (i-NWs) are regarded as ideal components of nanoelectronics to circumvent the limitations of conventional lithographic approaches.[13–15] The resistive switching behavior of various chemically synthesized i-NWs, such as ZnO,[16,17] Co_3O_4,[18] NiO,[19–24] and WO_x[25] has been investigated, but postgrowth alignment of these i-NWs precisely on a large area with individual control is still a difficult challenge.[26,27] No current technique can successfully align the conventional short i-NWs/nanotubes on a large scale with individual positioning and alignment control for this application. To avoid the complicated deposition and patterning processes of the oxide layer in conventional lithographic techniques and the alignment difficulty in current i-NW techniques, a novel technique is required.

We report here a simple, inexpensive, and rapid method to fabricate 2D arrays of perpendicularly aligned, individually conductive Cu-NWs with a nanometer-scale Cu_xO layer sandwiched at each cross point, by using an inorganic-nanowire-digital-alignment technique (INDAT) and a one-step reduction process. In this approach, the oxide layer is self-formed and patterned, so conventional deposition and lithography are not necessary. INDAT eliminates the difficulties of alignment and scalable fabrication that are encountered when using currently available techniques that use inorganic nanowires. This approach also has the advantage that it maintains all expensive metals in the final product, whereas in conventional approaches most of the deposited metal is peeled off. Fabricated arrays had reproducible resistive switching behavior, high on/off current ratio (I_{on}/I_{off}) ≈ 10^6 and extensive cycling endurance; these characteristics imply that each cross-point of the Cu-NW arrays functioned as individually addressable RRAM and confirm that the INDAT-produced Cu-NWs were individually electrical conductive.

INDAT prints arbitrarily long and continuous NWs with incorporated precursors on a large area with computer-digital-control to achieve designed i-NW patterns after removing the organic component, so long continuous Cu-NWs that are digitally aligned can be printed on a large area. This approach prints a solution of the compound precursor and polymer into compound-precursor-incorporated polymer NWs with computerized digital alignment and then converts them to desired oxide and metallic patterns (**Figure 1**). The NW precursor can be any compound that is miscible with polymers in solution. The polymer component can be easily removed by calcination or other processes to leave aligned oxide NWs. Metal-oxide NWs can be converted to metallic NWs by heating in a reducing atmosphere.

An electrohydrohynamic NW (e-NW) digital printer[28–30] is an important component of INDAT. This printer consists of an injector and a collector (Figure 1). The injector includes a syringe pump, a gas-tight syringe, a high-voltage supplier, and a nozzle tip. The collector is grounded and can be moved horizontally under computer control to adapt to the speed at which the NWs are printed onto it.

We demonstrate fabrication of Cu-NWs. Polyvinylpyrrolidone (PVP) (4.5 wt%) and copper trifluoroacetate (CTA) (11.5 wt%) were blended in a mixed solvent of dimethylformamide and tetrahydrofuran (1:1 wt%) then printed in lines using our home-built e-NW printer to form aligned polymer NW that incorporate compound precursors. Adjustment of polymer solution concentration, solution injection rate, electric field, nozzle-to-collector distance, and the collector's moving speed and directions enabled production of long, cylindrical, straight, continuous NWs with diameter ≈88 nm composed of PVP and CTA (Figure S1a,b, Supporting Information). Cu-NWs with diameter ≈80 nm were obtained by oxidizing the NWs in air at 500 °C for

Dr. W. Xu, Y. Lee, Dr. S.-Y. Min, Prof. T.-W. Lee
Department of Materials Science and Engineering
Pohang University of Science
and Technology (POSTECH)
Pohang, Gyungbuk 790-784, Republic of Korea
E-mail: twlee@postech.ac.kr
Prof. C. Park
Department of Materials Science and Engineering
Yonsei University
Seoul 120-749, Republic of Korea

DOI: 10.1002/adma.201503153

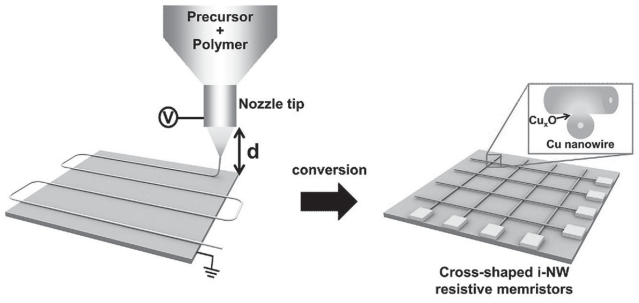

Figure 1. Schematic of the fabrication process of cross-shaped i-NW memristors. Left panel: Printing a solution of the compound precursor and polymer into well-aligned compound-precursor-incorporated NWs with digital control of the collector movement, and right panel: cross-shaped resistive memristors based on well-aligned i-NWs on a large area after the conversion processes.

1 h to remove organic components, then reducing the product in H_2 atmosphere at 300 °C (Figure S1c,d, Supporting Information). NW diameter can be controlled by adjusting the polymer solution concentration. A 15 m long NW can be produced in <2 min.[28] The NWs can be computer-digital aligned in a 20 cm × 20 cm area of the collector, which can be enlarged by remodeling the equipment. This is an inexpensive approach, especially for aligning expensive metals or oxides, because all metallic elements remain in the final product; this is an advantage over conventional lithography, which lifts off most of the coated metal.

Patterns of CTA-incorporated PVP-NWs can be printed by digitally controlling the tip-to-collector distance and the movement of the collector. Straight NWs, wavy NWs, and combinations of these forms can be obtained as shown in the scanning electron microscopy (SEM) images (**Figure 2**). The Cu-NW patterns were obtained after calcination and reduction (Figure S2, Supporting Information). Previously, several methods have

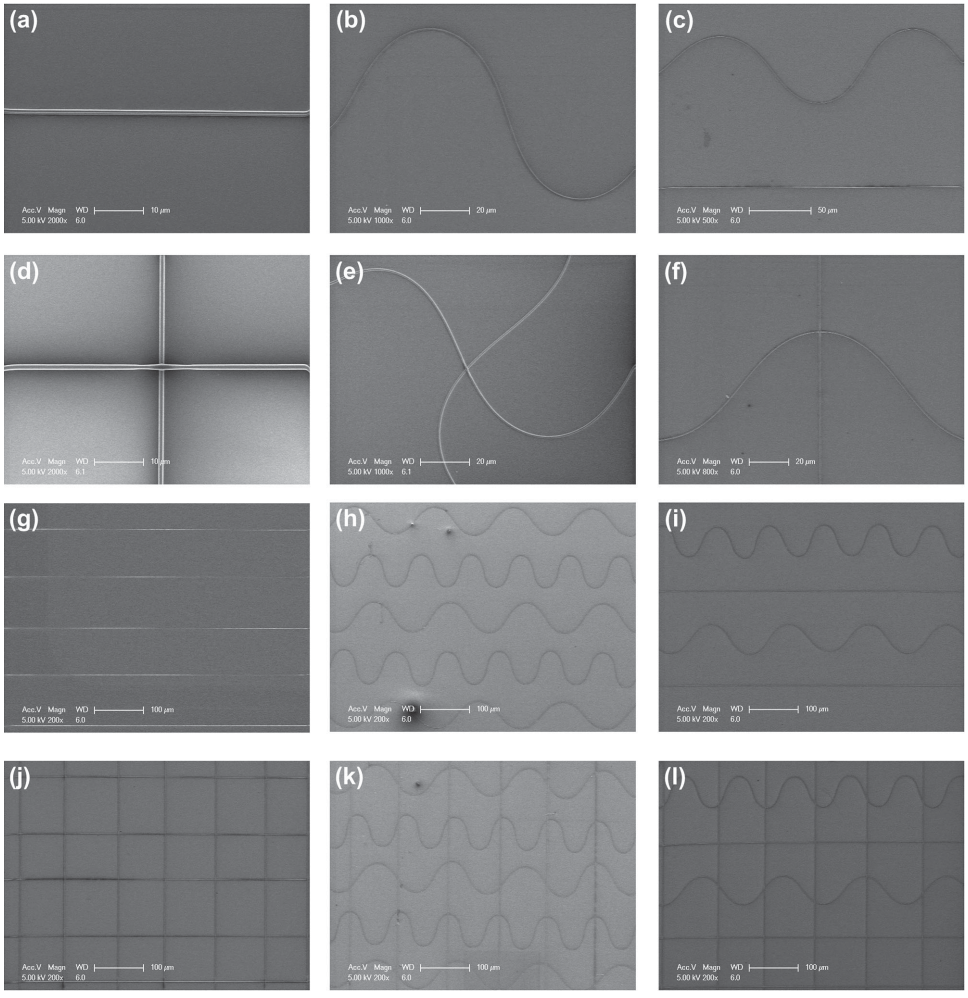

Figure 2. SEM images of some typical PVP-NW patterns that incorporate CTA. a) Single line, b) two crossing lines, c) parallel lines, d) grid lines, e) a wavy line, f) two crossing wavy lines, g) parallel wavy lines, h) grid of straight and wavy lines, i) parallel combination of straight and wavy lines, j) vertical combination of straight and wavy lines, k) wave-straight-wave-straight alignment, and l) grids of parallel NWs and wave-straight-wave-straight alignment.

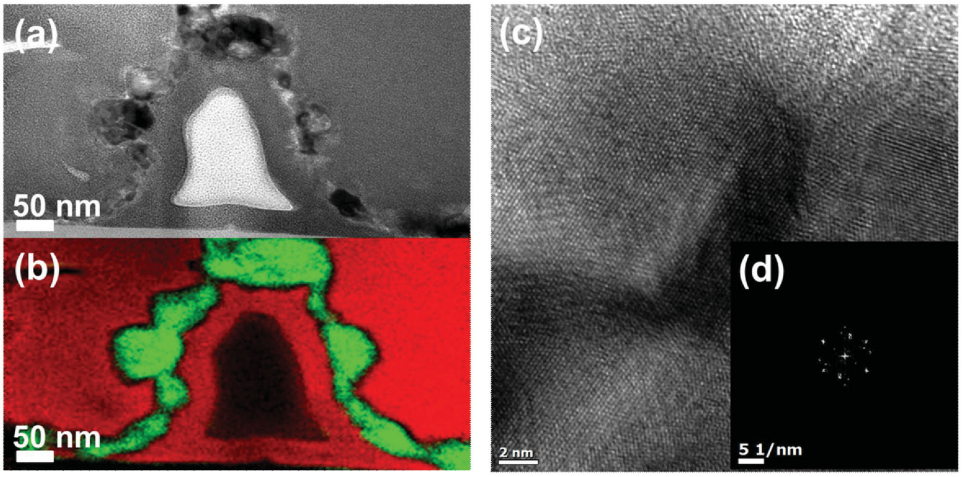

Figure 3. a) Transmission electron microscopy (TEM) image of cross-sectional view of single Cu-NW, b) electron energy loss spectroscopy (EELS) elemental mapping of (a) (green: Cu, red: C), e) TEM image of a magnified cross-sectional view of the Cu-NW, and d) crystallinity analysis of (c).

been proposed to assemble i-NWs after growing them[31,32] using self-assembly of block copolymers,[33] biorecognition,[34,35] shear forces,[36–45] magnetic, and electric fields,[26,46–48] but challenges remain, including overcoming a limited ability for lateral registration of the assembled NWs, assembling high-aspect-ratio NWs, achieving complex patterns of nanostructures, and most importantly, manipulating individual i-NWs instead of bundles of parallel i-NWs. Our approach can solve these difficulties. Compared to existing alignment techniques, INDAT is less expensive and faster; it is also scalable and can be digitally controlled. Moreover, wavy NWs are compatible with flexible electronics and therefore have potential to be used in next-generation stretchable devices, smart fabrics and wearable electronics.[49–51]

The Cu-NW is hollow (**Figure 3**a). During calcination, the organic components of the NW initially softened and decomposed; meanwhile, the NW started to collapse. Oxygen diffused into the NW from outside, and therefore the perimeter of the NW was primarily oxidized. At a certain moment, the inorganic components in the outer surface were mostly oxidized and oxides started to form a wall; at the same time, the inner organic components were converted to gaseous products. The gases tended to release through the wall. This gas-blow exerted a force that pushed inorganic components towards the wall and prevented it from fully collapsing, and finally resulted in formation of an inner hollow. After the NW was mostly oxidized, it hardened without collapse of the wall. The melting point of CuO (1326 °C) is much higher than the calculation temperature, and therefore the oxide shell remained rigid without further obvious change. This formation of hollow structures is comparable to that in electrospun NWs.[52,53] Cu was distributed around the central hollow (Figure 3b), and the Cu-NWs were polycrystalline (Figure 3c,d).

To evaluate conductivity of these Cu-NWs, two electrodes were deposited 3 mm apart along the Cu-NW. A voltage sweep was applied to one electrode and the other was grounded.

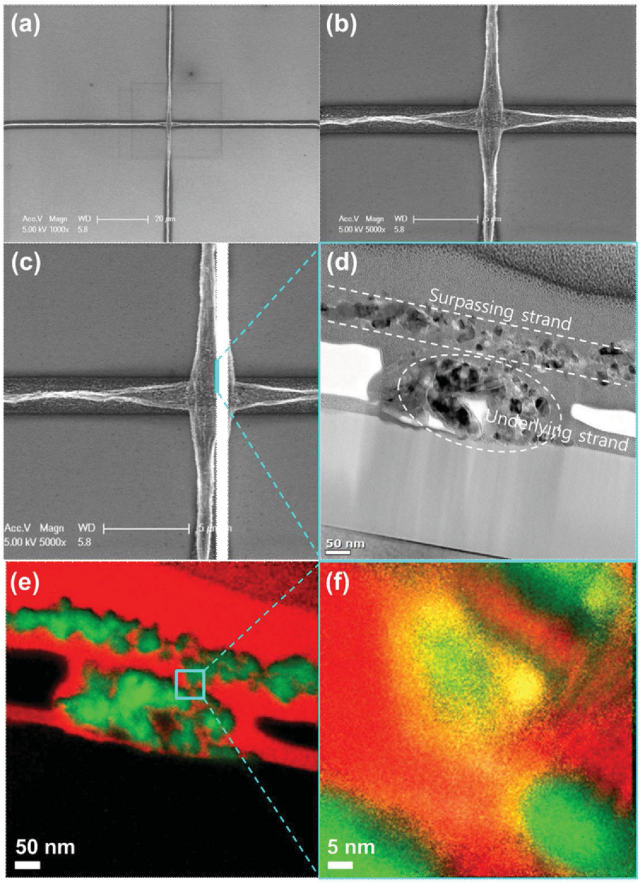

Figure 4. SEM images of a) two perpendicular Cu-NWs and b) magnified view of intersection. c) Indication of the position for focused-ion-beam cut. d) TEM image of cross-sectional view of two intersected strands, and e) relative elemental mapping by EELS (green: Cu; red: C; yellow: O), and f) EELS elemental mapping of a magnified TEM image of the connecting region of two intersected strands.

The continuity of the Cu-NW was evaluated by measuring the current as a function of the applied voltage (Figure S3, Supporting Information). No obvious electromigration effect that influences the conductivity of Cu-NWs was observed. Single Cu-NWs exhibited obvious metallic properties with a calculated conductivity of 8.15 S μm^{-1}, which is high enough for the NW to be used as a conductive line.

Applications of the cross-shaped Cu-NW arrays (Figure S1d, Supporting Information; Figure 5a) as RRAM devices are envisioned. Arrays of PVP-NWs that incorporated CTA were first fully oxidized in air at 500 °C for 1 h, then reduced in H_2 atmosphere at 300 °C for 2 h. Under H_2 atmosphere, a Cu_xO layer sandwiched between two crossed NWs would remain when the subsequent reduction conditions were carefully controlled, because the Cu_xO would be protected by the NWs. Then, a Cu–Cu_xO–Cu MOM sandwich structure could be formed and the interlayer Cu_xO could show resistive switching behavior. The fine structure of the intersection exhibited a # shape instead of being point-like (**Figure 4**a,b); each of the two perpendicular Cu-NWs separated into two strands (Figure 4b), and the resulting four strands intersected at four points to form a square. One point (Figure 4c, blue bar) was cut, then the cross-section was imaged (Figure 4d) and its elemental distribution was mapped (Figure 4e). A hollow structure was observed in the strand of the underlying Cu-NW (Figure 4d). In the fused region between the surpassing and underlying strands (Figure 4e), oxide was present (Figure 4f), i.e., a MOM structure formed. In conventional deposition-lithographic approaches, separate deposition and patterning of the oxide layer in the MOM structure requires special attention. Although previous work has yielded resistive switchable NWs, postaligning and precisely positioning them encountered severe difficulties.[13–25] In contrast, our approach does not require additional deposition and patterning or synthesis and positioning of the oxide structure but fabricates only bilayer Cu-NW electrodes with an oxide layer that is self-formed, self-patterned, and self-positioned by a simple one-step reduction process within the cross-points of Cu-NW grids.

To evaluate whether cross-shaped Cu-NW arrays work as a cross-point nonvolatile memory, their electrical properties (**Figure 5**a) were obtained by analysis of current–voltage (I–V) plots. Single-polar switching was observed (Figure 5b): during a bias sweep from 0 to 6 V, current level was initially low (high-resistance state (HRS)). When the voltage approached ≈4.5 V, the current abruptly increased; this "SET" process switched the inter-Cu_xO layer to the low-resistance state (LRS). Then as the voltage was swept again from 0 to ≈4.5 V, the current remained at the higher level of LRS; as the voltage was swept further from 4.5 to ≈12 V, the current suddenly dropped ("RESET") and the Cu_xO layer returned to the HRS. Repetitive sweeping cycles almost overlapped the first cycle; this result indicates that the operation state is reliable. At reading voltage of 1 V, the on/off current ratio was ≈10^6 (Figure 5b).

To analyze the conduction mechanisms, the I–V plots of HRS and LRS were redrawn (Figure S4a,b, Supporting Information). In the HRS, current density J (A m^{-2}) was well described by the Thermionic Emission conduction model[54]

$$J \propto T^2 \exp\left[\frac{-\left(\phi - q\sqrt{\frac{qV}{4d\pi\varepsilon}}\right)}{kT}\right] \quad (1)$$

where T (K) is the absolute temperature, ϕ (eV) is Schottky barrier height, $q = -1.602 \times 10^{-19}$ C is the charge on the electron,

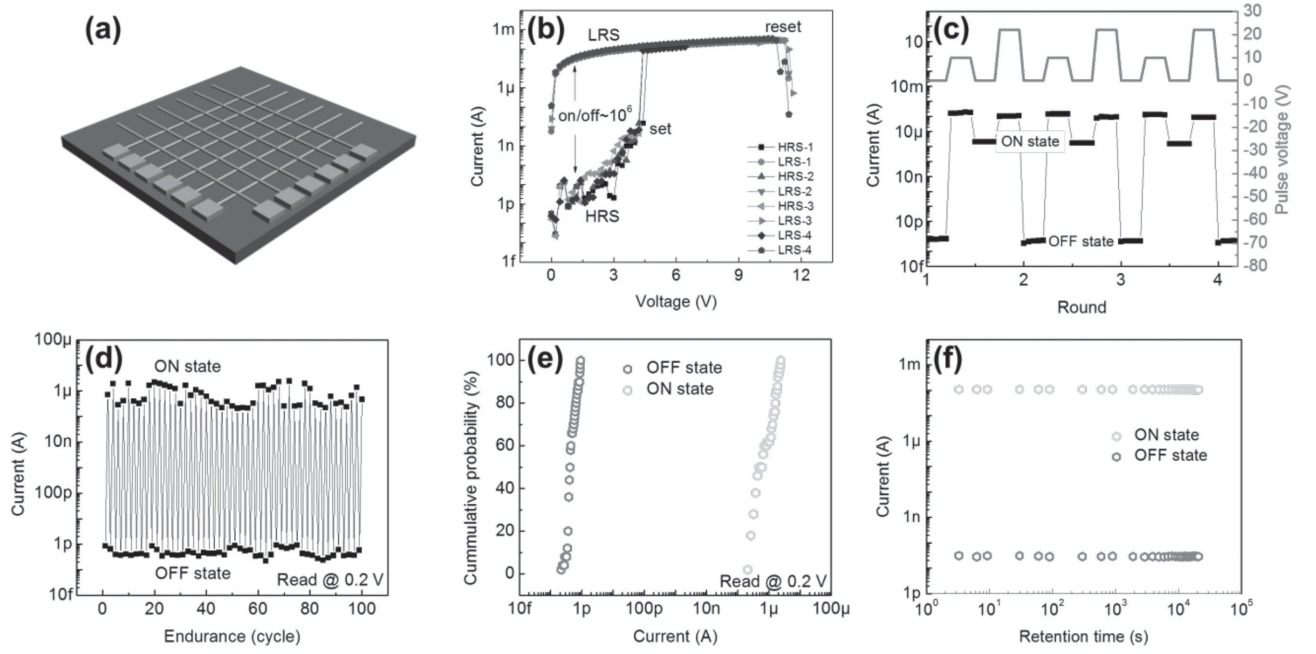

Figure 5. a) Schematic of cross-shaped Cu-NW resistive memristor arrays, b) plot of current as a function of sweeping voltage for the resistive switching behavior of a cross-shaped Cu-NW resistive memristor, c) sequential SET and RESET processes of the memristor, d) endurance cycles of the memristor, e) cumulative probability of ON/OFF currents that demonstrate clear separation of the two states, and f) retention of ON/OFF states of the memristor.

V (V) is the applied voltage, d (m) is the oxide thickness, ε (F m^{-1}) is the dielectric permittivity, and $k = 8.617 \times 10^{-5}$ eV K^{-1} is Boltzmann's constant. In the LRS, J was well described by the Ohmic conduction model

$$J \propto V \exp\left(\frac{-\Delta E_{ae}}{kT}\right) \quad (2)$$

where ΔE_{ae} (eV) is the change in activation energy of electrons.

Sequential SET and RESET processes can change the resistance of the Cu_xO interlayer to sufficiently distinct low or high values, which are regarded as "ON" or "OFF," respectively, in a memory device (Figure 5c). The currents of LRS and HRS were read at 0.2 V; the SET and RESET processes were reproduced for 100 cycles without degradation of the device (Figure 5d and Figure S5, Supporting Information). The cumulative probabilities (Figure 5e) indicate that they showed reliable function without current overlap of both ON and OFF currents for up to 100 cycles. Data retention was evaluated in a continuous reading process at 1 V. The on/off current ratio $\approx 10^6$ was maintained for $>2 \times 10^4$ s without any degradation (Figure 5f); this observation confirmed that the cross-shaped Cu-NW arrays functioned as individually addressable RRAM at each cross point, and that the Cu-NWs were individually electrical conductive.

We have reported a simple process to fabricate cross-shaped Cu-NW memristors using an inorganic-nanowire-digital-alignment technique and a one-step reduction process. The controllable alignment technique potentially solves the difficulties in aligning i-NWs to specified designs, enables rapid computer-designed alignment of arbitrarily long continuous i-NWs on a large area, and can produce versatile patterns including straight lines, wave lines, and any combination of these lines. Scalable production of Cu-NWs with various alignments was achieved. A simple one-step reduction process was used to obtain metal–oxide–metal structure at the cross points of rectangular Cu-NW grids. This simple process facilitates fabrication of cross-point nonvolatile memristor arrays. The memristors showed repeatable resistive switching behavior, a high on/off current ratio $\approx 10^6$ and stable data retention time for $>2 \times 10^4$ s. This technique is applicable to aligning broad classes of compound precursors that are miscible with polymers in a solution to generate i-NWs and is an economical approach that retains all metallic elements in the final product. This is the first report of memristors with the resistive switching oxide layer self-formed, self-patterned, and self-positioned; we envision that the new features of the technique will provide great opportunities for future nanoelectronic circuits.

Supporting Information

Supporting Information is available from the Wiley Online Library or from the author.

Acknowledgements

W.X. and Y.L. contributed equally to this work. This research was supported by the Pioneer Research Center Program through the National Research Foundation (NRF) of Korea funded by the Ministry of Science, ICT and Future Planning (2012-0009460). This work was also supported by the Center for Advanced Soft-Electronics funded by the Ministry of Science, ICT and Future Planning as Global Frontier Project (2014M3A6A5060947).
Note: The acknowledgements were updated on January 14, 2016, after initial publication online.

Received: June 30, 2015
Revised: September 12, 2015
Published online: November 20, 2015

[1] R. Waser, M. Aono, *Nat. Mater.* **2007**, *6*, 833.
[2] D. B. Strukov, G. S. Snider, D. R. Stewart, R. S. Williams, *Nature* **2008**, *453*, 80.
[3] G. I. Meijer, *Science* **2008**, *319*, 1625.
[4] D.-H. Kwon, K. M. Kim, J. H. Jang, J. M. Jeon, M. H. Lee, G. H. Kim, X.-S. Li, G.-S. Park, B. Lee, S. Han, M. Kim, C. S. Hwang, *Nat. Nanotechnol.* **2010**, *5*, 148.
[5] Y. Yang, P. Gao, S. Gaba, T. Chang, X. Pan, W. Lu, *Nat. Common.* **2012**, *3*, 732.
[6] P. Heremans, G. H. Gelinck, R. Müller, K.-J. Baeg, D.-Y. Kim, Y.-Y. Noh, *Chem. Mater.* **2011**, *23*, 341.
[7] Y. Ji, D. F. Zeigler, D. S. Lee, H. Choi, A. K.-Y. Jen, H. C. Ko, T.-W. Kim, *Nat. Commun.* **2013**, *4*, 2707.
[8] J. Yao, J. Lin, Y. Dai, G. Ruan, Z. Yan, L. Li, L. Zhong, D. Natelson, J. M. Tour, *Nat. Commun.* **2012**, *3*, 1101.
[9] J. J. Kim, B. Cho, K. S. Kim, T. Lee, G. Y. Jung, *Adv. Mater.* **2011**, *24*, 2104.
[10] S. Nau, C. Wolf, S. Sax, E. J. W. List-Kratochvil, *Adv. Mater.* **2015**, *27*, 1048.
[11] G. W. Burr, B. N. Kurdi, J. C. Scott, C. H. Lam, K. Gopalakrishnan, R. S. Shenoy, *IBM J. Res. Dev.* **2008**, *52*, 449.
[12] B. Cho, S. Song, Y. Ji, T.-W. Kim, T. Lee, *Adv. Funct. Mater.* **2011**, *21*, 2806.
[13] W. Lu, C. M. Lieber, *Nat. Mater.* **2007**, *6*, 841.
[14] Y. Cui, C. M. Lieber, *Science* **2001**, *291*, 851.
[15] D. J. Beesley, J. Semple, L. K. Jagadamma, A. Amassian, M. A. McLachlan, T. D. Anthopoulos, J. C. de Mello, *Nat. Commun.* **2014**, *5*, 3933.
[16] J. Park, S. Lee, J. Lee, K. Yong, *Adv. Mater.* **2013**, *25*, 6423.
[17] Y. Yang, X. Zhang, M. Gao, F. Zeng, W. Zhou, S. Xie, F. Ran, *Nanoscale* **2011**, *3*, 1917.
[18] K. Nagashima, T. Yanagita, K. Oka, M. Taniguchi, T. Kawai, J. S. Kim, B. H. Park, *Nano Lett.* **2010**, *10*, 1359.
[19] K. Oka, T. Yanagita, K. Nagashima, T. Kawai, J. S. Kim, B. H. Park, *J. Am. Chem. Soc.* **2010**, *132*, 6634.
[20] W. Z. Wu, Z. L. Wang, *Nano Lett.* **2011**, *11*, 2779.
[21] C. Cagli, F. Nardi, B. Harteneck, Z. Tan, Y. Zhang, D. Ielmini, *Small* **2011**, *7*, 2899.
[22] S. I. Kim, J. H. Lee, Y. W. Chang, S. S. Hwang, K.-H. Yoo, *Appl. Phys. Lett.* **2008**, *93*, 033503.
[23] K. Oka, T. Yanagida, K. Nagashima, H. Tanaka, T. Kawai, *J. Am. Chem. Soc.* **2009**, *131*, 3434.
[24] L. He, Z.-M. Liao, H.-C. Wu, X.-X. Tian, D.-S. Xu, G. L. W. Cross, G. S. Duesberg, I. V. Shvets, D.-P. Yu, *Nano Lett.* **2011**, *11*, 4061.
[25] S. Lee, J. Lee, J. Park, Y. Choi, K. Yong, *Adv. Mater.* **2012**, *24*, 2418.
[26] J. Yao, H. Yan, C. M. Lieber, *Nat. Mater.* **2013**, *8*, 329.
[27] S.-H. Choi, B.-H. Jang, J.-S. Park, R. Demadrille, H. L. Tuller, I.-D. Kim, *ACS Nano* **2014**, *8*, 2318.
[28] a) S.-Y. Min, T.-S. Kim, B. J. Kim, H. Cho, Y.-Y. Noh, H. Yang, J. H. Cho, T.-W. Lee, *Nat. Commun.* **2013**, *4*, 1773; b) Y. Lee, T. S. Kim, S.-Y. Min, W. Xu, S.-H. Jeong, H.-K. Seo, T.-W. Lee, *Adv. Mater.* **2014**, *26*, 8010.
[29] W. Xu, H.-K. Seo, S.-Y. Min, H. Cho, T.-S. Lim, C.-y. Oh, Y. Lee, T.-W. Lee, *Adv. Mater.* **2014**, *26*, 3459.

[30] W. Xu, T.-S. Lim, H.-K. Seo, S.-Y. Min, H. Cho, M.-H. Park, Y.-H. Kim, T.-W. Lee, *Small* **2014**, *10*, 1999.
[31] N. P. Dasgupta, J. Sun, C. Liu, S. Brittman, S. C. Andrews, J. Lim, H. Gao, R. Yan, P. Yang, *Adv. Mater.* **2014**, *26*, 2137.
[32] M. C. P. Wang, B. D. Gates, *Mater. Today* **2009**, *12*, 34.
[33] J. Chai, D. Wang, X. Fan, J. M. Buriak, *Nat. Nanotechnol.* **2007**, *2*, 500.
[34] J. K. N. Mbindyo, B. D. Reiss, B. R. Martin, C. D. Keating, M. J. Natan, T. E. Mallouk, *Adv. Mater.* **2001**, *13*, 249.
[35] M. Chen, L. Guo, R. Ravi, P. C. Searson, *J. Phys. Chem. B* **2006**, *110*, 211.
[36] Y. Huang, X. Duan, Q. Wei, C. M. Lieber, *Science* **2001**, *291*, 630.
[37] X. Duan, C. Niu, V. Sahi, J. Chen, J. Wallace Parce, S. Empedocles, J. L. Goldman, *Nature* **2003**, *425*, 274.
[38] G. Yu, A. Cao, C. M. Lieber, *Nat. Nanotechnol.* **2007**, *2*, 372.
[39] A. Tao, F. Kim, C. Hess, J. Goldberger, R. He, Y. Sun, Y. Xia, P. Yang, *Nano Lett.* **2003**, *3*, 1229.
[40] D. Whang, S. Jin, Y. Wu, C. M. Lieber, *Nano Lett.* **2003**, *3*, 1255.
[41] S. Acharya, A. B. Panda, N. Belman, S. Efrima, Y. A. Golan, *Adv. Mater.* **2006**, *18*, 210.
[42] S. Jin, D. Whang, M. C. McAlpine, R. S. Friedman, Y. Wu, C. M. Lieber, *Nano Lett.* **2004**, *4*, 915.
[43] Z. Fan, J. C. Ho, T. Takahashi, R. Yerushalmi, K. Takei, A. C. Ford, Y.-L. Chueh, A. Javey, *Adv. Mater.* **2009**, *21*, 3730.
[44] K. Takei, T. Takahashi, J. C. Ho, H. Ko, A. G. Gillies, P. W. Leu, R. S. Fearing, A. Javey, *Nat. Mater.* **2010**, *9*, 821.
[45] Q. Cao, H.-S. Kim, N. Pimparkar, J. P. Kulkarni, C. Wang, M. Shim, K. Roy, M. A. Alam, J. A. Rogers, *Nature* **2008**, *454*, 495.
[46] P. A. Smith, C. D. Nordquist, T. N. Jackson, T. S. Mayer, B. R. Martin, J. Mbindyo, T. E. Mallouk, *Appl. Phys. Lett.* **2000**, *77*, 1399.
[47] X. Duan, Y. Huang, Y. Cui, J. Wang, C. M. Lieber, *Nature* **2001**, *409*, 66.
[48] C. M. Hangarter, N. V. Myung, *Chem. Mater.* **2005**, *17*, 1320.
[49] J.-W. Han, M. Meyyappan, *AIP Adv.* **2011**, *1*, 032162.
[50] K. H. Cherenack, T. Kinkeldei, C. Zysset, G. Tröster, *IEEE Electron Device Lett.* **2010**, *31*, 740.
[51] T. Sekitani, U. Zschieschang, H. Klauk, T. Someya, *Nat. Mater.* **2010**, *9*, 1015.
[52] H. Xiang, Y. Long, X. Yu, X. Zhang, N. Zhao, J. Xu, *CrystEngComm* **2011**, *13*, 4856.
[53] J. Kong, H. R. Tan, S. Y. Tan, F. Li, S. Y. Wong, X. Li, X. Lu, *Chem. Commun.* **2010**, *46*, 8773.
[54] Z. Jin, G. Liu, J. Wang, *AIP Adv.* **2013**, *3*, 052113.